Journal of Alloys and Compounds 648 (2015) 467–473

Contents lists available at ScienceDirect

Journal of Alloys and Compounds

journal homepage: http://www.elsevier.com/locate/jalcom

Synthesis, characterization and evaluation of scintillation properties of Eu^{3+}-doped Gd_2O_3 obtained using PEG as precursor

Lorena P.B. Durante [a], Leonardo A. Rocha [a], Daniela P. dos Santos [a], Fernando O. Coelho [a], Marco A. Schiavon [a], Sidney José L. Ribeiro [b], Jefferson L. Ferrari [a, *]

[a] Laboratório de Materiais Inorgânicos Fotoluminescentes e Polímeros Biodegradáveis (LAFOP), Grupo de Pesquisa em Química de Materiais – (GPQM), Departamento de Ciências Naturais, Universidade Federal de São João Del Rei, Campus Dom Bosco, Praça Dom Helvécio, 74, 36301-160, São João Del Rei, MG, Brazil

[b] Instituto de Química, UNESP, P.O. Box 355, 14800-970, Araraquara, SP, Brazil

ARTICLE INFO

Article history:
Received 28 July 2014
Accepted 27 June 2015
Available online 2 July 2015

Keywords:
Photoluminescence
Scintillator
Rare earth
Polyethyleneglycol
Gadolinium oxide

ABSTRACT

This work reports on the synthesis of Eu^{3+}-doped Gd_2O_3 using PEG as an organic molecular precursor with 1, 3, 5, 7 e 10 mol% of Eu^{3+}. TGA and DTA analysis of the precursors obtained shows that the final materials are obtained at thermal treatment above 700 °C. Based on this information all materials were obtained after heat treatment at 900, 1000 and 1100 °C during 4 h in an oven under air atmosphere. XRD analysis showed that the materials obtained after heat-treatment presents a cubic crystalline structure assigned to the Gd_2O_3. Crystallite size and microstrain were evaluated using the Scherrer's equation and Williansom-Hall method, respectively, as a function of heat-treated temperature and Eu^{3+} concentration. Raman spectroscopy also showed the formation of the Gd_2O_3 phase, however, the absence of bands around 117 cm^{-1} in the spectra with higher Eu^{3+} concentration indicates that the insertion of this one in the host matrix promotes the breakdown of some chemical bonds of the matrix. Intense photoluminescence emission in the visible region with maximum localized around 611 nm under excitation at 255 nm with xenon lamp and with X-ray source were observed. The emissions observed were attributed to the intraconfigurational f–f transitions of Eu^{3+}. The lifetime values of the $^5D_0$ excited state were between 2.84 and 2.89 ms, indicating the location of Eu^{3+} in crystalline systems. This result demonstrates the potential application of the materials in systems for absorption in the ultraviolet region, solar cells, devices generated images and scintillation systems.

1. Introduction

Current research on materials with great photoluminescent properties provides challenges for development of new technologies in many areas, including electronics, photonics, imaging devices generators, optical amplification and detection, fluorescent detection in biomedical engineering and environmental control [1].

Among the materials that are promising for these applications, those that contain Rare Earth ions (RE^{3+}) in their compositions has special interest. Materials containing RE^{3+} have been studied and excellent photoluminescent results have been obtained due to upconversion [2–4] and downconversion [5–7] properties.

Depending on nature of the ions, the RE^{3+} present different intraconfigurational f–f transitions and can generate emission or/and absorption properties ranging from the X-ray, ultraviolet and visible to infrared region of the electromagnetic spectrum [8].

Among RE^{3+}, europium (Eu^{3+}) is a chemical element belonging to the class of lanthanide, found in oxidation states II and III, in which, the oxidation state III offers greater stability. The Eu^{3+} have the electron configuration *[Xe]-4f*^{6}. The bands present in the spectrum of emission of Eu^{3+} are very well known, and are derived from the transitions *f–f* attributed to the energy levels $^5D_0 \rightarrow {}^7F_J$ (in which $J = 0, 1, 2, 3, 4$, etc) [8]. The most intense emission band in the spectrum is located in the region around 612 nm, red region of the electromagnetic spectrum attributed to the transition $^5D_0 \rightarrow {}^7F_2$, known as a hypersensitive transition. This

* Corresponding author. Grupo de Pesquisa em Química de Materiais (GPQM), Universidade Federal de São João del Rei, Departamento de Ciências Naturais, Campus Dom Bosco, Praça Dom Helvécio, 74 – Fábricas, São João Del Rei – MG, Brazil.

E-mail addresses: ferrari@ufsj.edu.br, jeffersonferrari@gmail.com (J.L. Ferrari).

http://dx.doi.org/10.1016/j.jallcom.2015.06.239
0925-8388/

transition is directly dependent on electric dipole (ED) mechanism. This characteristic allows the Eu^{3+} to be used as a structural probe in several host matrix to understand with more detail about the chemical enviromental around of this one [9].

Due to these specific characteristics of Eu^{3+}, many efforts have been realized in order to manufacture optical devices by introducing RE^{3+} in many kind of host matrix. Many papers have been presented in the literature showing that Gd_2O_3 is a promising oxide for the application as a host matrix for doping with RE^{3+} due to its particular chemical properties, photochemical and good photothermal stability, and its low-energy phonons related to the Gd-O chemical bonding [10]. The Gd_2O_3 is a versatile material with high potential for application in many fields of technology ranging from the development of corrosion-resistant coatings, due to their thermal stability and refractory properties and scintillation properties.

The incorporation of RE^{3+} into crystalline matrix contribute to the appearance of many kind of imperfections that may affect negatively the photoluminescence spectroscopic properties. The presence of defects and/or microstrains in crystalline structures, can contribute to the appearance of processes that affect directly on photoluminescence process via non-radiative mechanisms. These processes deactivate the excited state in which promotes the reduction of lifetime values, and consequently compromises the quantum yield of the system.

In this sense the present work reports on preparation of Eu^{3+}-doped Gd_2O_3 via molecular polymeric route using polyethyleneglycol (PEG) as a precursor. The photoluminescent, structural and scintillation properties were evaluated in order to ascertain their potentialities for applications in technological devices.

2. Material and methods

Eu^{3+}-doped Gd_2O_3 with 1, 3, 5, 7 and 10 mol% in powder form were prepared through the polymerization using polyethyleneglycol (PEG) as precursor. Gd_2O_3 and Eu_2O_3 were dissolved in an aqueous medium containing concentrated hydrochloric acid to obtain the standard solution, to be used as precursor solution in preparation of all samples. These standard solutions were titrated with EDTA 0.01 mol L^{-1} at room temperature. Five precursor's solution were obtained, where each solution containing the exact ratio of Eu^{3+} (1, 3, 5, 7 and 10 mol%) in relation to mol amount of Gd^{3+} were prepared as follow: The exact volume of each solution containing Eu^{3+} and Gd^{3+} was pipetted into a beaker (Solution 1). Into another container, the mass of PEG was added corresponding to 10 times the sum of the moles of both metals ([Gd^{3+}+Eu^{3+}]) and dissolved in deionized water (Solution 2). Then both solutions were mixed, Solution 1 and Solution 2. The mixed solutions were kept under stirring, approximately 150 rpm at 80 °C to obtain the viscous solution called precursors solutions. The thermal behavior of all the precursors solutions with different concentrations of Eu^{3+} were analyzed by Thermogravimetric Analysis (TGA) and Differential Thermal Analysis (DTA) using the thermobalance Shimadzu, model DTG-60H under synthetic air atmosphere under heating rate of 10 °C/min, from 25 up to 1000 °C. Based on thermal behavior observed, the precursor solutions were heat-treated at 900, 1000 and 1100 °C for 4 h in an oven (EDG model 1800) under an air atmosphere. During the heat-treatment, the conditions were kept the same as those used during TGA and DTA analysis. The materials obtained after the heat treatments were characterized by X-Ray diffraction (XRD), operating a Shimadzu diffractometer, K_α of Cu radiation, $\lambda = 1.5418$ Å, graphite monochromator, step of 0.02 degrees between $2\theta = 10°–80°$. Based on the diffractograms obtained, the Scherrer's equation was used to estimate the crystallite size of crystal structure and the microstrains were evaluated by Willianson-Hall (W–H) method. The materials were also characterized by Raman spectroscopy using Raman spectrophotometer LabRam-HR with excitation source at 632.8 nm. Photoluminescence properties were carried out at room temperature using a Fluorolog spectrofluorometer SPEXF2121/Jobin-Yvon with excitation source at 255 nm, with filter cut-off bellow 399 nm. The excitation and emission slits were 5 and 2 nm, respectively. The decay curves of the excited state of the materials were obtained using a Fluorolog spectrofluorometer SPEXF2121/Jobin-Yvon with excitation and emission fixed at 255 nm and 611 nm, respectively. The excitation and emission slits, were the same reported above. The samples were crushed in an agate mortar with 100 mg of KBr, and submitted under a pressure of 10 tons for 1 min to obtain the pellets. The pellets were characterized by Fourier Transform Infra-Red (FTIR) spectroscopy operating a Perkin Elmer spectrometer (Spectrum GX) in transmission mode recording 32 spectrums with a resolution of 4 cm^{-1}. For the emission spectra under X-ray excitation was used the X-ray diagnostic equipment with 100 kV (energy 100 kev) ma CR 100 − 7/100 − SHR, optical fiber with 400 microns localized at 3 mm from the sample and a spectrometer Sovereign UV/Visible. The frequency energy used is around 2.2×10^{19}.

3. Results and discussion

Fig. 1(A) and (B) show TGA analysis showing the efficiency of sintering and the elimination of species from the organic compound, PEG, used as precursors. As seen in Fig. 1(A), the process for obtaining material takes place in four stages, in which both

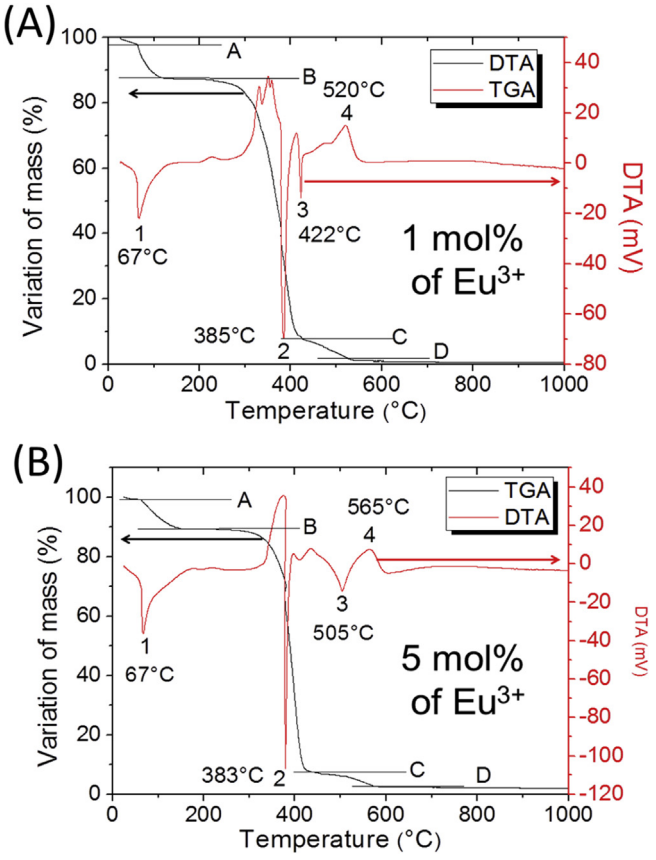

Fig. 1. TGA/DTA analysis of precursors viscous solutions containing Eu^{3+}: A) 1 and B) 5 mol% from room temperature up to 1000 °C.

endothermic and exothermic events. The first loss of mass of about 12% occurs in approximately 67 °C and can be attributed to the loss of water present in the precursor solutions. The second step, at about 385 °C, as well the third stage (between 420 and 510 °C), show significant loss of mass around 80%. The weight loss is attributed to the elimination of organic matter from PEG used as precursor in the synthesis of materials [11]. At approximately 520 °C, an endothermic peak in a single step is assigned to the elimination of residues still present, presumable from organic matter strongest linked on surface of material formed. The formation of Gd_2O_3 crystalline phase can be obtained in temperatures above 700 °C, because any endothermic or exothermic events and loss of mass is observed in this range. Increasing the concentration of Eu^{3+}, Fig. 1(B), thermal behavior remains the same even where it is observed in the same steps. The total loss of mass for full formation of material, approximately 98%, is due to the full elimination of the PEG precursor. A large mass of PEG was used in these work to promote a maximum homogeneity among metals as possible in precursor solution to promote the composition of the final material to be well dispersed. Thus, this detail can contributes to the homogeneous distribution of RE^{3+} in the final material in order to obtain a maximum efficiency of photoluminescent properties. To make sure no residue of organic matter present in the final material, heat-treatment temperatures that the samples were submitted were 900, 1000 and 1100 °C.

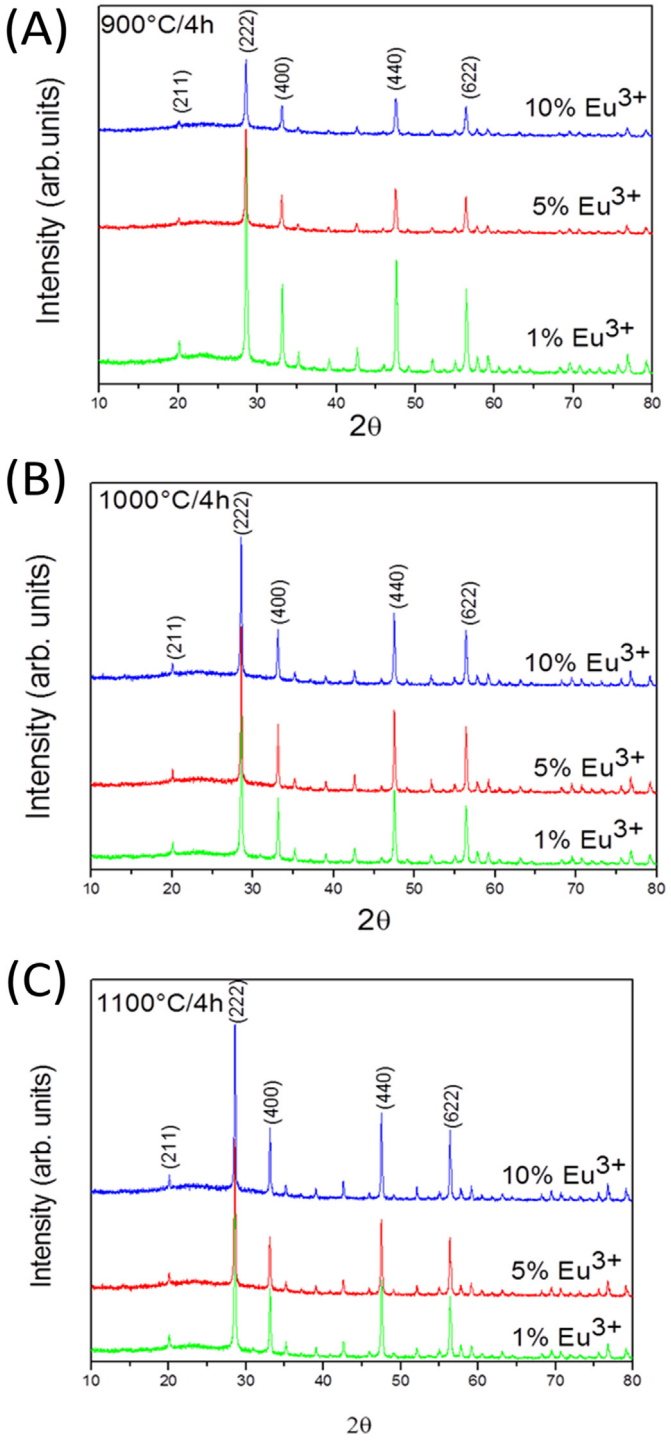

Fig. 2. Diffractograms of Eu^{3+}-doped materials heat-treated at: (A) 900 °C, (B) 1000 °C and (C) 1100 °C for 4 h in air atmosphere.

From the analysis of XRD was possible to evaluate the crystallinity of the materials obtained at different heat-treatments, and Fig. 2(A)–(C) show the XRD patterns of the materials obtained at 900, 1000 and 1100 °C. According to the XRD patterns obtained, all materials are well crystalline. The reflections observed were assigned to the (hkl) planes with Miller indices equal: (211), (222), (400), (440) and (622) located at $2\Theta = 20.1°$, 28.6°, 33.1°, 47.5° and 56.4°, respectively. The planes observed are atributted to the cubic crystal structure of Gd_2O_3 in accordance to the JCPDF cards number 00-012-0797. No other phase was observed in the diffractograms with different concentrations of Eu^{3+}, and temperatures of obtaining, indicating that this route promotes the insertion of this ion into the matrix of Gd_2O_3 with quite easily. Based on the diffraction patterns of the samples heat-treated at 900 and 1100 °C, the average crystallite size by Scherrer's equation (Equation (1)) were determined. In the Scherrer's equation, D is the crystallite size, K is the shape factor and this work was used 0.89, λ is the wavelength of X-Ray radiations used in the analysis (Cu° $K_\alpha = 1.5418$ Å), and the β in the Full Width Half Maximum (FWHM) of the most intense reflection, and in this case we used the reflection assigned to the (222) planes located at $2\Theta = 28.6°$ [12].

$$D_{hkl} = \frac{K\lambda}{\beta\cos\theta} \quad (1)$$

The crystallite size values are shown in Table 1. The microstrains were determined using Williansom-Hall as described in Equation

Table 1
Crystallite size values obtained by the Scherrer's equation.

Heat-treatment temperature (°C)	Samples (mol% of Eu^{3+})	Crystallite size (nm)
900	1	34.8
	5	38.16
	10	29.13
1100	1	35
	5	44.53
	10	40.32

Table 2
Microstrain obtained by Williamson-Hall.

Heat-treatment temperature (°C)	Samples (mol% of Eu^{3+})	Microstrains ($\times 10^{-3}$)
900	1	1.04
	5	1.34
	10	1.12
1100	1	1.30
	5	1.10
	10	1.15

(2). Initially this method consists in plotting a graph of 4senθ along the *x*-axis along $\beta_{hkl}\cos\theta$ the *y*-axis. From a linear fit to the data, the ε microstrain is obtained from the slope of the fit [13].

$$\beta_{hkl}\cos\theta = \frac{K.\lambda}{D} + 4\varepsilon\ \sin\theta \quad (2)$$

The microstrain values obtained are shown in Table 2 and do not show significant differences each other. This may be related to the stability of the crystallite size. Another important point that need to be taken into account is that the presence of Eu^{3+} does not promote significant changes in the crystalline structure of Gd_2O_3. The values of the ionic radii for the Gd^{3+} and Eu^{3+} with coordination number values equal to 6 are 1.078 Å and 1.087 Å, respectively. The similarity between the ionic radii for both ions favors the inclusion of large amounts of Eu^{3+} within the Gd_2O_3 structure without bringing significant changes in the crystalline system.

The materials obtained at higher temperatures of heat-treatment, 1100 °C, were submitted to FTIR analysis, and the results are shown in Fig. 3. These samples have been chosen because in previous work it was observed that at higher temperatures of heat-treatment, there is a lower presence of −OH, or other groups that acts like photoluminescence quenchers. All materials presents bands at 410 cm^{-1} and 540 cm^{-1} that can be associated with the chemical bonding stretching of νGd-O groups [14,15]. This is an indication of the formation of Gd_2O_3 solid network. Bands localized around 3400 cm^{-1} are assigned to the stretching of O—H groups. These groups are still present in the samples heat-treated at 1100 °C for 4 h, but increasing the Eu^{3+} concentration promotes the decreasing of the intensity of this band. Thus, the presence of this ion can contribute to the elimination of this species.

The bands located around 1525 and 1397 cm^{-1} are assigned to the stretching of the C=O and C—O groups, respectively. These groups may have been formed during the heat-treatment in which the atmosphere contains carbon released during organic precursor decomposition and could be forming bonds with O^{2-} localized on surface of the Gd_2O_3 particles. The bands localized around 1710 cm^{-1} can be assigned to the carboxyl groups. In accordance to the Nakamoto, 1986, the carboxyl groups have vibrational stretching mode localized between 1730 e 1700 cm^{-1} [16]. These bands indicate the presence of these species located on surface of the Eu^{3+}-doped Gd_2O_3 particle. Vibration mode of species like C=O and C—O groups and carboxyl can be observed basicaly only by FTIR analysis. Although the TG and DTA analysis show the complete

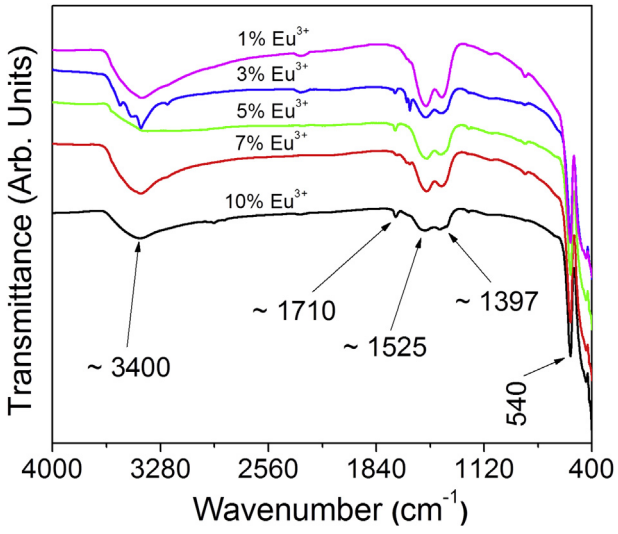

Fig. 3. FTIR spectra of Eu^{3+}-doped Gd_2O_3 obtained at 1100 °C for 4 h.

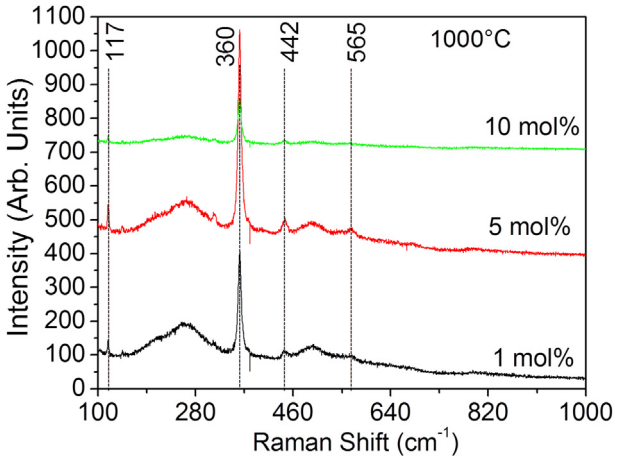

Fig. 4. Raman Spectra of Eu^{3+}-doped Gd_2O_3 obtained at 1000 °C with 1, 5 and 10 mol %.

decomposition of organic matter and obtaining of Gd_2O_3 crystalline phase occurs above 700 °C.

The Fig. 4 show the Raman spectra of sample heat-treated at 1000 °C. The bands localized at 117, 360, 442 and 565 cm^{-1} are associated to the cubic phase of Gd_2O_3 compatible to commercial oxide of the same phase [17]. These results also show the formation of a single crystalline phase of Gd_2O_3 oxide without the presence of secondary phases. The more intense band at about 360 cm^{-1} is associated with $E_g + F_g$ mode being the most intense band of the cubic phase with space group Ia_3 stage (206) of Gd_2O_3 [18,19] corresponds to the results obtained and showed in this work by XRD. The intensity of band located at 117 cm^{-1} changes as a function of Eu^{3+}. This indicates that this ion may be causing a little change in the chemical bonds, but does not cause significant changes in spectroscopic and structure properties.

The materials obtained were submitted to photoluminescence spectroscopy under excitation source at 255 nm. The photoluminescence emission spectra are show in Fig. 5(A), (B) and (C). All samples containing Eu^{3+} showed an intense red emission observed by naked eye and the transitions attributed to the $^5D_0 \rightarrow {}^7F_J$ (J = 0, 1, 2, 3, 4). All transitions observed in the emission spectra are characteristic of Eu^{3+} with the most intense band localized around 611 nm ascribed to transition $^5D_0 \rightarrow {}^7F_2$. This transition is allowed by the electric dipole (ED) and only occurs when the Eu^{3+} ions are located in the site of symmetry with absence of inversion center (*i*). The band localized around 581 nm is assigned to the $^5D_0 \rightarrow {}^7F_0$ transition. The bands localized between 585 and 603 nm are assigned to the transitions $^5D_0 \rightarrow {}^7F_1$ of the Eu^{3+}. This band is assigned to the transition of Eu^{3+} allowed by the magnetic dipole (MD), where the intensity of this transition does not depend on environment where the RE^{3+} is localized. The bands located between 645 and 670 and the band located between 681 and 719 are assigned to the $^5D_0 \rightarrow {}^7F_3$ and $^5D_0 \rightarrow {}^7F_4$, respectively. It appears that the materials obtained here exhibit an intense absorption in the ultraviolet region which is converted to intense emission in the red region. It can be observed in Fig. 6 that samples with higher relative emission intensity, though not as intense as others, were those heat-treated at 1100 °C.

The decay curves of the excited state of the transition $^5D_0$ were also obtained fixing the excitation and emission at 255 and 611 nm, respectively. Fig. 7 shows the decay curve of the sample containing 7 mol% of Eu^{3+} heat treated at 1100 °C that is representative for all samples obtained in this work. The values obtained are shown in Table 3. The decay curves were fitted to a first

order exponential decay with values of R of around 0.999. The values of lifetime were between 2.84 and 2.89 ms noting that there was no great change with increasing of Eu^{3+} concentration in the system, as well as with increasing temperature heat-treatment. Practically it is not observed change in the values of lifetime. This effect can be related to the low microstrain observed in this work and also the similarity of ionic radii between Eu^{3+} and Gd^{3+}, causing no significant changes in the crystal lattice. Even if the materials showed groups such as O–H, C–H, C=H, and carboxyl groups, which act as a deactivator excited states of the RE^{3+}, showed intense photoluminescence emission and relative long lifetime values of the excited state $^5D_0$ of the Eu^{3+} in the materials obtained here. Lifetime values obtained suggest that the Eu^{3+} are located inside of the crystal lattice, protected from the groups located on particle surface

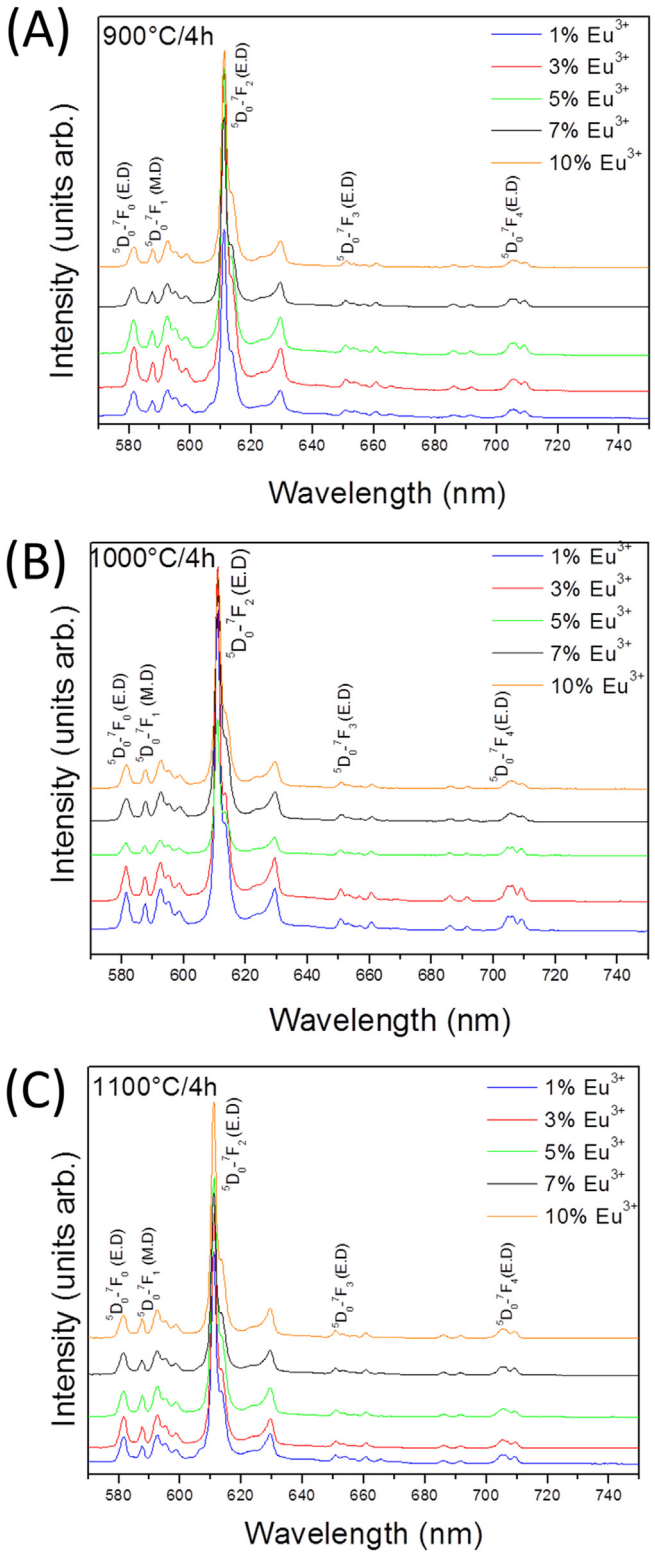

Fig. 5. Photoluminescence emission spectra of Eu^{3+}-doped Gd_2O_3 heat treated at (A) 900, (B) 1000 and (C) 1100 °C for 4 h under excitation at 255 nm.

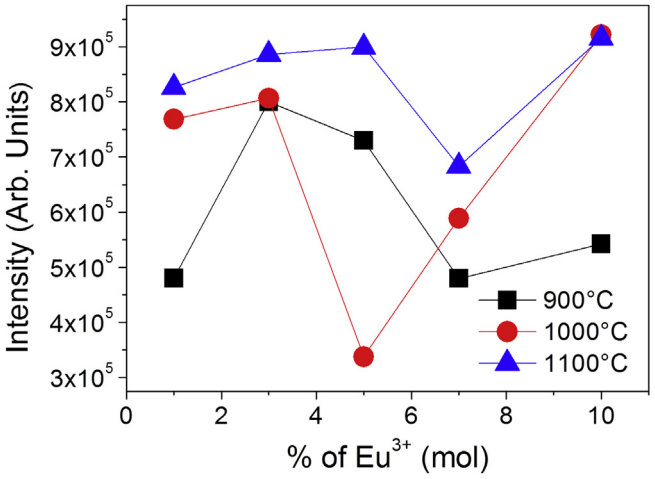

Fig. 6. Maximum intensity of photoluminescence on the transition $^5D_0 \rightarrow {}^7F_2$ of the materials obtained.

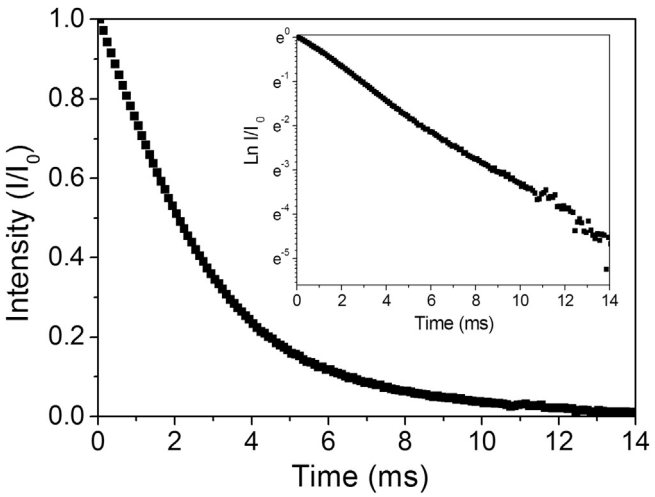

Fig. 7. Photoluminescence decay curve of $^5D_0$ excited state of Eu^{3+}–Gd_2O_3 heat-treated at 1100 °C for 4 h.

Table 3
Lifetime values of the excited state $^5D_0$.

Heat-treatment temperature (°C)	Samples(mol% of Eu^{3+})	Lifetime (ms)
900	1	2.88
	5	2.86
	10	2.85
1100	1	2.87
	5	2.84
	10	2.89

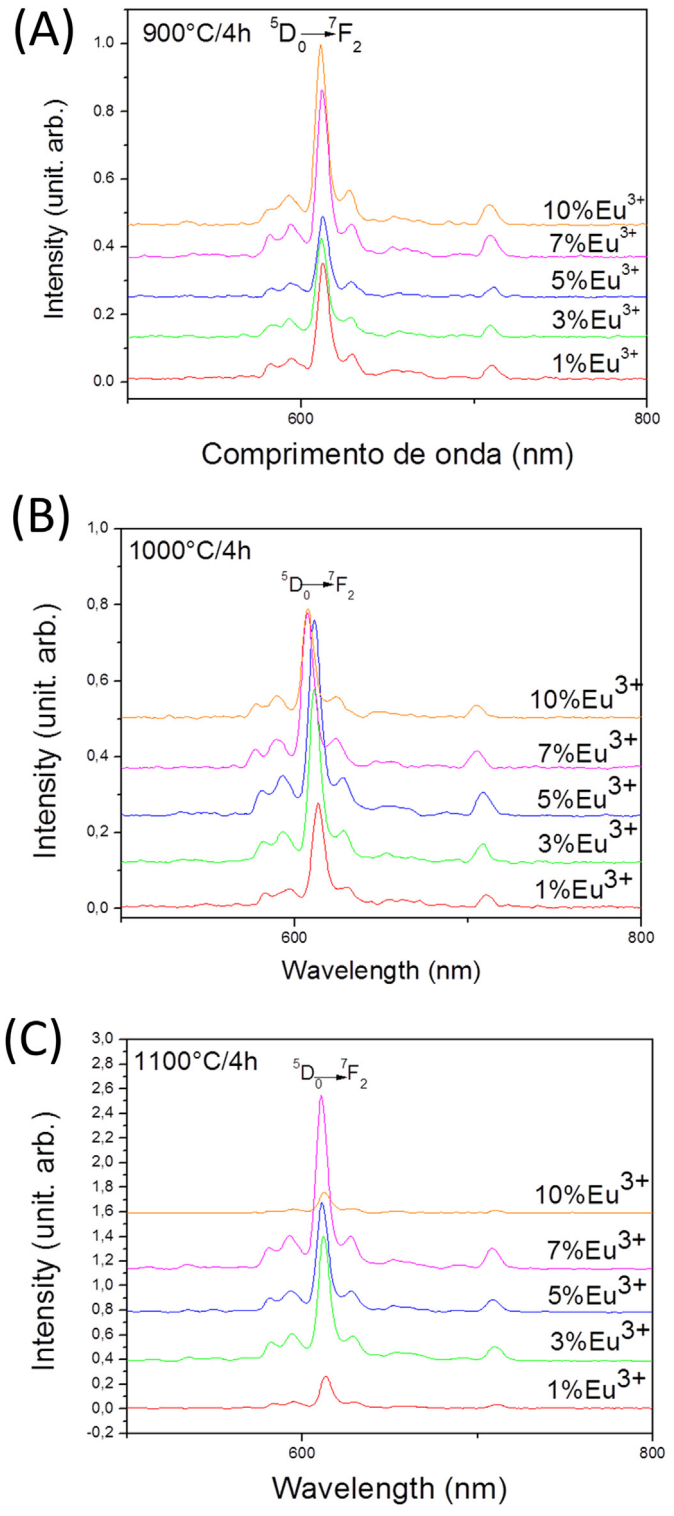

Fig. 8. Photoluminescence emission spectra of Eu^{3+}-doped Gd_2O_3 heat treated at (A) 900, (B) 1000 and (C) 1100 °C for 4 h under excitation with X-ray source.

avoiding loss via non-radiative process.

In order to evaluate the possibility of application as a scintillator, the materials obtained were excited using X-rays radiation, and the results are shown in Fig. 8(A)–(C). All materials when excited with X-ray source showed intense emission in the red region assigned to the Eu^{3+} transitions. The most intense emission is located at 611 nm associated with the transition $^5D_0 \rightarrow {}^7F_2$

4. Conclusions

In summary the results showed that the route chosen for obtaining these materials was success. The heat-treatment temperature chosen showed significant results on the formation of the crystalline phase of the materials. The heat-treatment temperatures do not have significant impact on the values of microstrain and on the crystallites size. The concentrations of Eu^{3+} added in the system also no caused structural variation assigned to the similarity between the ionic radii of the Eu^{3+} and Gd^{3+}. Even the presence of functional groups and species that may contribute to the deactivation of the excited state still maintained an intense photoluminescence and long lifetime values of the excited state, suggesting the inclusion of RE^{3+} within the host matrix protects it from groups located on surface. When the material was excited by X-ray radiation, intense emission in the red region was observed, suggesting that this material has potential for application in scintillators devices.

Acknowledgments

The authors would like to acknowledge FAPEMIG, FAPESP, CAPES, and CNPq. This work is a collaboration research project of members of the Rede Mineira de Química (RQ-MG) supported by FAPEMIG (Project: REDE-113/10). The authors also acknowledge Jenifer Esbenshade for English revisions.

References

[1] G. Blasse, B.C. Grabmaier, Luminescent Materials, Springer-Verlag, Berlin, 1994.
[2] R.V. Perrella, D.P. dos Santos, G.Y. Poirier, M.S. Góes, S.J.L. Ribeiro, M.A. Schiavon, J.L. Ferrari, Er^{3+}-doped Y_2O_3 obtained by polymeric precursor: synthesis, structure and upconversion emission properties, J. Lumin 149 (2014) 333–340.
[3] J.L. Ferrari, K. de Oliveira Lima, E. Pecoraro, R.A.S. Ferreira, L.D. Carlosc, R.R. Gonçalves, Color tunability of intense upconversion emission from Er^{3+}–Yb^{3+} co-doped SiO2–Ta_2O_5 glass ceramic planar waveguides, J. Mater. Chem. 22 (2012) 9901–9908.
[4] J.L. Ferrari, K.O. Lima, L.J.Q. Maia, S.J.L. Ribeiro, A.S.L. Gomes, R.R. Gonçalves, Broadband NIR emission in Sol–Gel Er^{3+}-Activated SiO_2–Ta_2O_5 glass ceramic planar and channel waveguides for optical application, J. Nanosci. Nanotechnol. 11 (2011) 2540–2544.
[5] L.A. Rocha, M.A. Schiavon, C.S. Nascimento Jr., L. Guimarães, M.S. Góes, A.M. Pires, C.O. Paiva-Santos, O.A. Serra, M.A. Cebim, M.R. Davolos, J.L. Ferrari, Sr_2CeO_4: Electronic and structural properties, J. Alloy Compd. 608 (2014) 73–78.
[6] J.L. Ferrari, M.A. Cebim, A.M. Pires, M.A. Couto dos Santos, M.R. Davolos, Y_2O_3:Eu^{3+} (5 mol%) with Ag nanoparticles prepared by citrate precursor, J. Solid State Chem. 183 (2010) 2110–2115.
[7] J.L. Ferrari, A.M. Pires, O.A. Serra, M.R. Davolos, Luminescent and morphological study of Sr_2CeO_4 blue phosphor prepared from oxalate precursors,, J. Lumin 131 (2011) 25–29.
[8] O.L. Malta, Theoretical crystal-field parameters for the YOC1-Eu^{3+} system – A simple overlap model, Chem. Phys. Lett. 88 (1982) 353–356.
[9] K. Driesen, V.K. Tikhomirov, C. Gorller-Walrand, Eu^{3+} as a probe for rare-earth dopant site structure in nano-glass-ceramics, J. Appl. Phys. V. 102 (2007) 24312.
[10] J.L. Ferrari, R.L.T. Parreira, A.M. Pires, S.A.M. Lima, M.R. Davolos, A route to obtain Gd_2O_3:Nd^{3+} with different particle size, Mater. Chem. Phys. 127 (2011) 40–44.
[11] H. Guo, N. Dong, M. Yinm, L. Lou, S. Xia, Visible upconversion in rare earth ion-Doped Gd_2O_3 Nanocrystals, J. Phys. Chem. B 108 (2004) 19205–19209.
[12] Li-Ling Ooi, Principles of X-ray Crystallography, Oxford University Press, Oxford, 2010.
[13] V.D. Mote, Y. Purushotham, B.N. Dole, Willianson-Hall analysis in estimations of lattice strain in nanometer-sized ZnO particles, J. Theor. Appl. Phys. 6 (2012) 1–8.
[14] N. Dhananjaya, H. Nagabhushana, B.M. Nagabhushana, B. Rudraswamy, C. Shivakumara, R.P.S. Chakradhar, Hydrothermal synthesis, characterization and Raman studies of Eu^{3+} activated Gd_2O_3 nanorods, Phys. B 406 (2011) 1639–1644.
[15] N. Dhananjaya, H. Nagabhushana, B.M. Nagabhushana, B. Rudraswamy, C. Shivakumara, R.P.S. Chakradhar, Spherical and rod-like Gd_2O_3:Eu^{3+} nanophosphors—structural and luminescent properties, Bull. Mater. Sci. 35 (2012) 519–527.
[16] K. Nakamoto, Infrared and Raman Spectra of Inorganic and Coordination

Compounds, fifth ed., John Wiley & Sons, Inc., New York, 1997.
[17] A. García-Murillo, A. Le Luyer, C. Dujardin, C. Pedrini, J. Mugnier, Elaboration and characterization of Gd_2O_3 waveguiding thin filmes prepareted by the sol-gel process, Opt. Mater. 16 (2001) 39–46.
[18] G. Rajan, K.G. Gopchandran, Engineering of luminescence from Gd2O3:Eu3+ nanophosphors by pulsed laser deposition, Opt. Mat. 32 (2009) 121–132.
[19] G. Rajan, K.G. Gopchandran, Enhanced luminescence from spontaneously ordered $Gd_2O_3:Eu^{3+}$ based nanostructures, Appl. Surf. Sci. 255 (2009) 9112–9123.